Available online at www.sciencedirect.com
ScienceDirect
Bioorganic & Medicinal Chemistry 15 (2007) 3515–3523
Bioorganic & Medicinal Chemistry

Regulatory molecules for the 5-HT$_3$ receptor ion channel gating system

Satoshi Yoshida,* Takashi Watanabe and Yasuo Sato*

Pharmaceutical Research Department, Meiji Seika Kaisha Ltd, 760, Morooka-Cho, Kohoku-ku, Yokohama 222-8567, Japan

Received 4 January 2007; revised 23 February 2007; accepted 27 February 2007
Available online 7 March 2007

Abstract—Substituted benzoxazole derivatives which possess a nitrogen-containing heterocycle at C2 are selective partial agonists of the 5-HT$_3$ receptor. Alteration of substituents on the benzoxazole nucleus affords both agonist-like and antagonist-like compounds, and uniquely modifies the function of the 5-HT$_3$ receptor ion channel gating system. SAR and corroborative computational docking study for these partial agonists successfully explained structure and function of the 5-HT$_3$ receptor.

1. Introduction

The serotonin type 3 (5-HT$_3$) receptor is one of the ligand-gated ion channel (LGIC) receptors that mediate critical synaptic transmission in both the peripheral and central nervous systems.[1] The nicotinic acetylcholine receptor (nACh), GABA$_A$ receptor, and ionotropic glycine receptor are classified into this family, and functional failure of these receptors causes a variety of chronic diseases. For decades, small-molecular ligands which interact with and modulate the functions of LGIC receptors have been recognized as candidate therapeutic agents. For example, 5-HT$_3$ receptor antagonists, such as granisetron (**3**, Figure 1) and alosetron (**4**, Figure 1), have widely been used for the treatment of chemotherapy-induced emesis and irritable bowel syndrome (IBS).[2–4] However, the structures and functions of LGIC receptors remain obscure. Because the crystal structure of LGIC receptors has not been determined, the following two approaches have mainly been used to investigate their structure and function. (1) Structure–activity relationship (SAR) studies of LGIC receptor ligands:[5] SAR data are particularly valuable to investigate receptor functions, which are difficult to predict even from crystallographic data. (2) Modeling based on homology with related proteins:[6,7] the acetylcholine binding protein (AChBP) possesses high amino acid sequence homology with LGIC subunits, and its 3D structure has been determined at high-resolution from crystallographic data.

We have reported that the benzoxazole derivatives **1** (Figure 1), which possess a nitrogen-containing heterocycle at C2, are selective partial agonists of the 5-HT$_3$ receptor.[8–11] The most distinctive feature of our compounds is the substituent-dependence of their effects on the 5-HT$_3$ receptor ion channel, that is, modification of substituents (R^1, R^2) on the rigid benzoxazole nucleus of **1** affords both agonist-like and antagonist-like compounds. As in the case of the endogenous agonist serotonin (5-HT, **2**, Figure 1), an agonist-like compound possessing high intrinsic

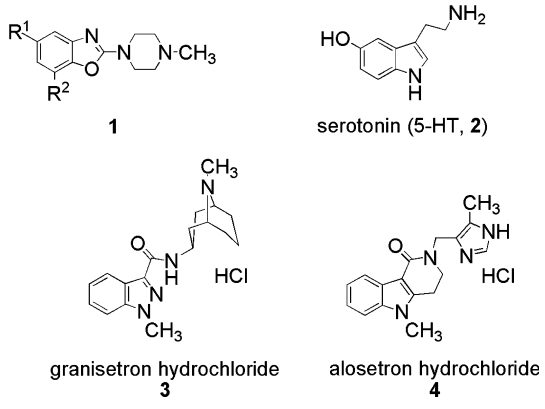

Figure 1. 5-HT$_3$ receptor ligands.

Keywords: 5-HT$_3$ receptor; LGIC; Partial agonist; Ion channels; Molecular modeling.
* Corresponding authors. Tel.: +81 45 541 2521; fax: +81 45 541 0667 (S.Y.); e-mail addresses: satoshi_yoshida@meiji.co.jp; yasuo_sato@meiji.co.jp

0968-0896/$ - see front matter © 2007 Elsevier Ltd. All rights reserved.
doi:10.1016/j.bmc.2007.02.054

activity (ia) stabilizes the open state of the ion channel and allows influx of Na^+ into the cytoplasm. On the other hand, an antagonist-like molecule with low ia decreases the frequency of channel-opening and the permeability of ions. Herein, we present SAR data for our 5-HT_3 receptor partial agonists corroborated with a computational docking study between our ligands and a homology-modeled guinea pig 5-HT_3 receptor. The results not only provide a basis for rational design of novel 5-HT_3 receptor ligands with high affinity and desirable ia, but also offer information about structural and functional aspects of the LGIC receptors. In particular, the substrate-dependence of the ia of these partial agonists provides clues to the roles of the amino acid residues in the ligand-binding region of the receptor.

2. Results and discussion

Compounds **1a**–**z** were synthesized by means of the procedures illustrated in Scheme 1. All compounds substituted at the 5 or/and 7 positions of the benzoxazole ring were synthesized from *o*-nitrophenols. Reduction of **5b**–**z** by catalytic hydrogenation followed by ring formation with carbon disulfide afforded the cyclized thiols **7b**–**z** in good yield. Coupling of **7b**–**z** with *N*-methylpiperazine was achieved by means of the following methods: (i) Coupling of *N*-methylpiperazine with 2-chlorobenzoxazole obtained by the reaction of 2-mercaptobenzoxazole with phosphorus pentachloride. (ii) Heating a mixture of 2-mercaptobenzoxazole and *N*-methylpiperazine in a nonpolar solvent. Compound **1a** was obtained by the treatment of commercially available 2-chlorobenzoxazole with *N*-methylpiperazine.

All of the biological data were obtained from contraction tests using isolated guinea pig ileum:[9] The activity of each compound for the 5-HT_3 receptor is represented by the parameter pD_2 and the intrinsic activity (ia). The pD_2 value indicates the order of agonist potency, expressed as the inverse logarithm of the half-maximal effective concentration (EC_{50}) of a partial agonist, that is, the concentration at which the biological–response curve reaches 50% of the maximal response. The value of ia represents the relative efficacy of a partial agonist as compared to the full agonist 5-HT (ia = 1.0, Table 1), that is, this parameter relatively quantifies the intensity of agonist-induced signal transduction. To avoid overlooking compounds that possess affinity for the receptor, but exhibit a low ia (antagonist-like molecules), ability to block the effect of 10^{-5} M 5-HT (5-HT_3 antagonism) was also measured. The binding profile of representative compounds with 5-HT_3 receptor and the selectivity over other receptors are presented in supplementary data (Tables S1 and S2). Homology model building of the guinea pig 5-HT_3 receptor was carried out with Insight II (Accelrys, San Diego, CA) and Cerius2 (Accelrys) on the basis of the crystal structure of AChBP.[12,13] Docking simulations were performed with Cerius2 based on the crystal structures of AChBP complexed with nicotinic acetylcholine (nACh) ligands.[12,13] We hypothesized that the characteristic ammonium moiety of LGIC ligands (protonated form) commonly interacts with the highly conserved amino acid residue of LGIC receptors, because all reported crystal structures of AChBP complexed with nACh ligands indicate a close contact between the ammonium moiety of nACh ligands and a carbonyl-oxygen of Trp147 in the AChBP, which is highly conserved among LGIC receptors.[14] Numerous SAR studies and mutational studies on LGIC receptors have demonstrated the importance of the ammonium moiety for interaction with the receptor, and the crucial role of the conserved Trp residue for ligand binding.[10,15,16] Based on the presumption, the ligand location was constrained during calculation such that the quaternary ammonium salt of the ligand was positioned near the carbonyl oxygen of Trp183 in the 5-HT_3 receptor binding region; this residue corresponds to Trp147 in the AChBP.

Table 1 summarizes the activity of the compounds. The ia data of **1a**–**m** in Table 1 indicate that modification of the C5 substituent (R^1) moderately varied the agonist/antagonist-like characteristics of the compounds. Introducing an electron-donating group, such as CH_3, OCH_3 or NH_2 (compds **1b**, **1f**, and **1g**), at C5 afforded partial agonists with high ia (>0.7), but introduction of an electron-withdrawing substituent, NO_2, Cl, or Br (**1e**, **1i**, and **1j**), yielded partial agonists with lower ia (around 0.5 or less). The variable ia of the compounds depending on the C5 substituent may be dependent upon whether the C5 substituent directly contacts the receptor amino acid residues that play a role in ion channel gating, or whether it indirectly influences the electrostatic character of a distant functional group having contacts with such residues. The pD_2 data of these compounds indicate that alteration of the C5 substituent can change the agonist potency of the compounds for the 5-HT_3 receptor over 10-fold. Small lipophilic C5 substituents, such as CH_3, F, Cl, and Br (compds **1b** and **1h**–**j**, Table 1), notably increased the pD_2 of the compounds. Other C5 substituents with greater steric hindrance, Et (**1c**) and tBu (**1d**), and with hydrophilicity, OCH_3(**1f**), NH_2(**1g**), CF_3(**1k**), $COCH_3$(**1l**), and CO_2Et (**1m**), did not increase pD_2. Both the low pD_2 and the weak 5-HT_3 antagonism of these compounds reflect their weak affinity for the receptor. These groups may undergo steric and/or electrostatic repulsion with amino acid residues in the binding site. On the other hand, the observation that small lipophilic C5 substituents afford compounds with both superior pD_2 and potent antagonism indicates that the C5 substituent may fit in a narrow, hydrophobic groove of the binding region in the receptor. In the case of C7 substituents (R^2 compds **1n**–**r**, Table 1), the type of functional group on C7 has a marked effect on ia, but little effect on pD_2. Introduction of a CH_3 group at C7 provided an agonist-like compound **1n** with high ia, while Et and Cl groups at the same position afforded antagonist-like compounds **1o** and **1r** with low ia (ia = 0.15 for **1o** and 0.24 for **1r**) without any change of pD_2. Compound **1p**, which has an exceptionally bulky substituent (*i*-Pr), showed unmeasurably low pD_2 and ia, but showed good antagonism (81%) at 10^{-5} M; this suggests that **1p** can be classified as a full antagonist. Furthermore, the low ia of the C7 chlorinated compound **1r** suggests that not only the steric, but also the electrostatic characteristics of the C7

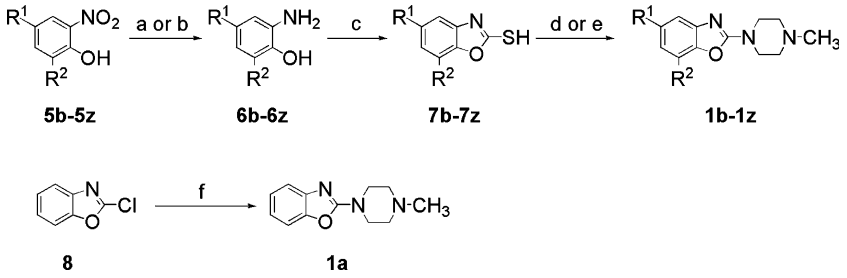

Scheme 1. Synthesis of **1a**–**z**. (a) H_2, Pd/C, EtOH; (b) H_2, Pt on sulfide carbon, EtOH; (c) CS_2, KOH, EtOH, reflux; (d) i.PCl_5, toluene, reflux; ii.N–Me piperazine, toluene; (e) N–Me piperazine, toluene, reflux; (f) N–Me piperazine, chloroform.

Table 1. Agonist activity of **1a**–**z** for the 5-HT_3 receptor

Compound	R^1	R^2	ia ± SEM[a]	pD_2 ± SEM[a]	Antagonist %
1a	H	H	0.62 ± 0.12	5.01 ± 0.13	82
1b	CH_3	H	0.72 ± 0.04	6.00 ± 0.05	87
1c	Et	H	—[b]	<4.0	63
1d	*t*-Bu	H	—[b]	<4.0	47
1e	NO_2	H	0.52 ± 0.05	6.10 ± 0.10	79
1f	OCH_3	H	0.78 ± 0.05	4.78 ± 0.09	74
1g	NH_2	H	0.76 ± 0.05	4.97 ± 0.08	73
1h	F	H	0.64 ± 0.04	5.57 ± 0.06	91
1i	Cl	H	0.50 ± 0.03	6.07 ± 0.15	92
1j	Br	H	0.48 ± 0.03	6.21 ± 0.04	89
1k	CF_3	H	—[b]	<4.0	36
1l	$COCH_3$	H	—[b]	<4.0	22
1m	CO_2Et	H	—[b]	<4.0	28
1n	H	CH_3	0.58 ± 0.06	5.48 ± 0.06	89
1o	H	Et	0.15 ± 0.04	5.48 ± 0.13	90
1p	H	*i*-Pr	—[b]	<4.0	81
1q	H	OCH_3	—[b]	<4.0	57
1r	H	Cl	0.24 ± 0.15	5.50 ± 0.13	90
1s	CH_3	CH_3	0.62 ± 0.12	6.32 ± 0.13	94
1t	CH_3	Et	0.26 ± 0.02	6.46 ± 0.06	99
1u	CH_3	Cl	0.26 ± 0.06	6.22 ± 0.08	96
1v	CH_3	OCH_3	0.56 ± 0.09	6.13 ± 0.04	91
1w	Cl	CH_3	0.24 ± 0.07	6.70 ± 0.04	94
1x	Cl	Et	0.17 ± 0.03	6.82 ± 0.20	100
1y	Cl	Cl	0.14 ± 0.03	6.51 ± 0.04	90
1z	Cl	OCH_3	0.62 ± 0.07	6.16 ± 0.03	92
2			1.00	5.34 ± 0.02	—
3			—[b]	<4.0	100

[a] Standard error of the mean ($n = 5$).
[b] No agonistic response was observed at 10^{-4} M.

substituent might influence ia. To test this conjecture, compound **1q**, which carries a methoxy group at C7, was also synthesized. If the electrostatic character of the C7 group is important for ia, introduction of a strongly electron-donating substituent, in contrast to the electron-withdrawing Cl group, should raise the ia of the partial agonists. However, **1q** showed only weak antagonism (57%) at 10^{-5} M and agonistic activity was not detected. In order to improve the potency of the C7-substituted derivatives, we examined 5,7-disubstituted partial agonists. The pD_2 and ia data of compounds **1s**–**z** show that they possess greater potency than C7-substituted compounds, while the C7 substituent effect is retained. A bulky ethyl group (**1t**, **1x**) or an electronegative Cl group (**1u**, **1y**) at C7 lowered the ia in both the C5 CH_3 and the C5 Cl series, but the small, electron-donating CH_3 group retained the ia of **1s**. Compound **1w**, which possesses a Cl atom at C5 and a CH_3 group at C7, exhibited a lower ia (0.24) than we had expected. However, the substituent effect of the CH_3 group is still retained (compare the ia of **1w** with that of **1x** or **1y**). Finally, the introduction of a methoxy group at the C7 position of 5,7-disubstituted derivatives greatly enhanced the intrinsic activity of **1v** (ia = 0.56) and **1z** (ia = 0.62) with high pD_2, as we had anticipated. This result demonstrates that the electrostatic character of the C7 substituent influences the ia of partial agonists in a similar manner to that of the C5 substituent. The modest impact of the C7 substituent on pD_2 and the strong influence on ia imply that the receptor amino acid residues that interact with the C7 substituent play little role in ligand binding, but have an important role in

ion channel gating, and in particular, sterically bulky C7 substituents are likely to show a greater interaction with the gating amino acid residues.

Figure 2a and b shows the result of docking of **1a** with the homology-modeled guinea pig 5-HT_3 receptor. The quaternary ammonium group of **1a** forms hydrogen bonds with the oxygen functions of Trp183 and Asp228, and has a cation-π interaction with Phe235. The aromatic ring of **1a** is intercalated, and is involved in hydrophobic interaction with Leu184 and Tyr153. The piperazine ring also interacts hydrophobically with the aromatic side chains of Trp183 and Phe235. The O1 oxygen of **1a** can form a hydrogen bond with Ser231. The N3 nitrogen atom is directed toward Asn138, Ile139, Tyr141, and may form hydrogen bonds with these residues through water. This model can explain the SAR data for our compounds. The structurally inflexible β-sheets involving Val142 and Tyr143 are located extremely close to the C5 substituent, and form a narrow hydrophobic space. This is consistent with the strong preference for a small substituent at C5 for high pD_2. In contrast, bulky and/or hydrophilic C5 substituents would have a repulsive interaction with these amino acid residues on the β-sheets. The benzoxazole nucleus of **1a** sandwiched between Leu184 and Tyr153 may have a π–π interaction with the side-chain aromatic ring of Tyr153. The SAR study on the C5 substituent showed that small electron-withdrawing substituents, such as F, Cl or Br, are favorable for high pD_2. We conjecture that the introduction of those groups into the benzoxazole ring of **1a** lowers its LUMO level, and intensifies the π–π interaction between **1a** and electron-rich Tyr153. The exceptionally good pD_2 of the NO_2 (**1e**) group despite its polarity can also be explained by the compactness and strongly electron-withdrawing character of this group. We previously proposed a '3-point pharmacophore model' for agonist binding to the 5-HT_3 receptor.[9] This model consists of an aromatic ring, a nitrogen atom in a heteroaryl group, and terminal amine as essential functions. Our docking model has allowed us to visualize putative interactions between these ligand structural features and amino acid residues in the 5-HT_3 receptor model. In considering the variation of ia of our partial agonists, the observed interaction between O1 oxygen and Ser231 is particularly important. Ser231 corresponds to Cys191 on loop C of AChBP, and this residue is associated with distinct conformational changes upon binding of agonists as compared with antagonists (Fig. 2c). This domain appears to play a critical role in ion channel gating by the LGIC receptors.[12,13] The introduction into ligands of C5 and C7 substituents with different electrostatic character alters the electron density of the O1 oxygen and the strength of the hydrogen bond between O1 oxygen and Ser231: C5 and C7 substituents with electron-donating character increase the electron density of the O1 oxygen and form a stronger hydrogen bond with the OH group of Ser231. This interaction stabilizes the 'closed' conformation (agonist binding form of AChBP, in which the ion

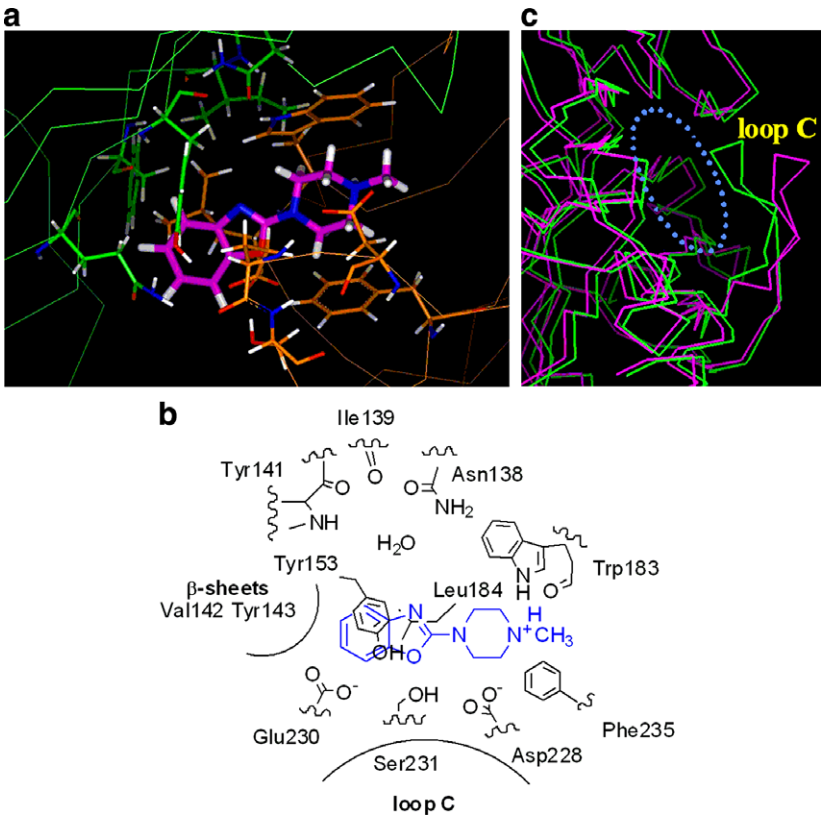

Figure 2. (a and b) Docking model of **1a** with 5-HT_3 receptor ligand binding domain. (c) Agonist and antagonist binding forms of the homology-modeled 5-HT_3 receptor. The ligand binding domain (light blue dotted frame), 'closed' conformation (green), and 'open' conformation (magenta) are shown.

channel is activated; Fig. 2c).[12] On the other hand, substituents with electron-withdrawing character decrease the electron density of the O1 oxygen atom and weaken the hydrogen bond. Binding of these ligands rather stabilizes the 'open' conformation (antagonist-binding form of AChBP, in which the ion channel is deactivated; Fig. 2c).[12] Our model indicates that a substituent at C7 can also interact with loop C. The above SAR data show that a sterically bulky C7 substituent dramatically lowers the ia of the partial agonists. We can interpret this in terms of steric repulsion between the bulky C7 substituent and the amino acid residues on loop C, causing the receptor to favor the 'open' conformation. Thus, our findings indicate that the variable ia of our partial agonists principally originates from the diverse character of the interactions between the compounds and loop C of the 5-HT_3 receptor.

3. Conclusion

In summary, we have shown that synergy between biochemical and computational docking studies can greatly aid interpretation of SAR data for 5-HT_3 receptor ligands. Our results will be useful for the rational design of 5-HT_3 receptor partial agonists with desirable ia and good potency, and demonstrate the effectiveness of docking calculations with experimental constraints. The characteristic substrate-dependence of the ia of our partial agonists allowed us to elucidate the roles of various amino acid residues in the ligand binding region, as well as throwing light on the structural features of the 5-HT_3 receptor. We are currently using a similar approach to design novel ligands for other LGIC receptors.

4. Experimental

4.1. Chemistry

Elemental analysis data were recorded on VarioEL (Elementar). NMR spectra were obtained on JEOL GX-400 FT-NMR spectrometers. The following abbreviations are used: s = singlet, d = doublet, t = triplet, q = quartet, quin = quintet, m = multiplet, and br = broad. MS were measured with Hitachi M-80B and JEOL JMS-700 instruments. Serotonin (**2**) and granisetron (**3**) are commercially available products.

4.1.1. 2-(4-Methyl-1-piperazynyl)benzoxazole (1a). 2-Chlorobenzoxazole (**8**; 1.4 g, 9 mmol) was added to the solution of 1-methylpiperazine (1 g, 10 mmol) in chloroform (100 ml) at 0 °C. The reaction mixture was stirred for 30 min and then the reaction quenched in ice-water (150 ml). The resulting mixture was extracted with ethyl acetate (200 ml), and the extract was dried over $MgSO_4$. After concentration in vacuo, the residue was chromatographed on silica gel with chloroform–methanol (20:1) and then recrystallized from water-acetone to give **1a** (1.8 g, 85%) as a white needle, mp 37–38 °C. NMR ($CDCl_3$ δ: 2.37 (3H, s, CH_3–), 2.54 (4H, t, J = 8 Hz, piperazine –CH_2– ×2), 3.73 (4H, t, J = 8 Hz, piperazine –CH_2– ×2), 7.02 (1H, t, J = 7 Hz, benzoxazole 5-H), 7.18 (1H, t, J = 7 Hz, benzoxazole 6-H), 7.26 (1H, d, J = 7 Hz, benzoxazole 7-H), 7.37 (1H, d, J = 7 Hz, benzoxazole 4-H). MS (EI) m/z 217 (M^+). Anal. Calcd for ($C_{12}H_{15}N_3O$): C, 66.34; H, 6.96; N, 19.34. Found: C, 66.46; H, 7.01; N, 19.08.

4.1.2. 5-Chloro-2-(4-methyl-1-piperazynyl)benzoxazole (1i). This procedure illustrates the general synthetic method for **1b**, **1d**, **1e**, and **1n**. 2-Amino-4-chlorophenol (**6i**; 10 g, 70 mmol) was refluxed for 8 h with potassium hydroxide (4.7 g, 84 mmol) and carbon disulfide (100 ml) in ethanol (150 ml). The reaction mixture was concentrated in vacuo. 1 N aqueous hydrochloric acid (100 ml) and ethyl acetate (200 ml) were added to the residue. The organic layer was washed with water, then dried over $MgSO_4$, and concentrated in vacuo. The 11.5 g of 5-chloro-2-mercaptobenzoxazole (**7i**) was obtained as a yellow powder and used in the next reaction without further purification. Phosphorus pentachloride (1.35 g, 6.5 mmnol) was added to the solution of **7i** (1 g, 5.4 mmol) in dry toluene (50 ml) at ambient temperature. The reaction mixture was refluxed for 1 h, then cooled in an ice bath. 1-Methylpiperazine (5.4 g, 54 mmol) was added dropwise to the mixture, and stirred for 30 min at 0 °C. The reaction mixture was diluted with chloroform (100 ml), then washed with water. The organic layer was dried over $MgSO_4$ and concentrated in vacuo. The residue was chromatographed on silica gel with chloroform–methanol (20:1) to afford **1i** (1 g, 67% from **5i**) as a white needle, mp 118–119 °C (acetone–hexane). NMR (CD_3OD) δ: 2.34 (3H, s, CH_3–), 2.57 (4H, t, J = 5 Hz, piperazine –CH_2– ×2), 3.71 (4H, t, J = 5 Hz, piperazine –CH_2– ×2), 7.03 (1H, d, J = 7 Hz, benzoxazole 6-H), 7.22 (1H, s, benzoxazole 4-H), 7.26 (1H, d, J = 7 Hz, benzoxazole 7-H). MS (EI) m/z 251 (M^+). Anal. Calcd for ($C_{12}H_{14}N_3OCl$): C, 61.26; H, 6.00; N, 17.86. Found: C, 61.21; H, 5.99; N, 17.87.

4.1.3. 5-Methyl-2-(4-methyl-1-piperazinyl)benzoxazole (1b). Obtained as yellow plate, 73% yield from 2-amino-*p*-cresol, mp 63–64 °C (methanol–ether). NMR ($CDCl_3$) δ: 2.35 (3H, s), 2.39 (3H, s), 2.52 (4H, t, J = 5 Hz), 3.71 (4H, t, J = 5 Hz), 6.82 (1H, d, J = 8 Hz), 7.11 (1H, d, J = 8 Hz), 7.15 (1H, s). MS (EI) m/z 231 (M^+). Anal. Calcd for ($C_{13}H_{17}N_3O$-1/8 H_2O): C, 66.86; H, 7.44; N, 17.99. Found: C, 66.77; H, 7.40; N, 18.00.

4.1.4. 5-tert-Butyl-2-(4-methyl-1-piperazynyl)benzoxazole (1d). Obtained as yellow oil, 62% yield from 2-amino-4-*tert*-butylphenol. NMR ($CDCl_3$) δ: 1.39 (9H, s), 2.42 (3H, s), 2.60 (4H, t, J = 4 Hz), 3.81 (4H, t, J = 4 Hz), 7.15 (1H, dd, J = 2, 8 Hz), 7.24 (1H, d, J = 8 Hz), 7.50 (1H, d, J = 2 Hz). MS (EI) m/z 274 (M^++1). Anal. Calcd for ($C_{16}H_{23}N_3O1/3H_2O$) C, 68.79; H, 8.54; N, 15.04. Found: C, 68.81; H, 8.67; N, 15.13.

4.1.5. 2-(4-Methyl-1-piperazynyl)-5-nitrobenzoxazole (1e). Obtained as yellow solid, 5% yield from 2-amino-4-nitrophenol, mp 112–113 °C (Et_2O–hexane).

NMR ($CDCl_3$) δ: 2.37 (3H, s), 2.56 (4H, t, J = 5 Hz), 3.80 (4H, t, J = 5 Hz), 7.32 (1H, d, J = 9 Hz), 8.13 (1H, d, J = 2 Hz), 8.18 (1H, dd, J = 2, 9 Hz). MS (EI) m/z 263 (M^++1). Anal. Calcd for ($C_{12}H_{14}N_4O_3$) C, 54.96; H, 5.38; N, 21.36. Found: C, 54.98; H, 5.23; N, 21.07.

4.1.6. 7-Methyl-2-(4-methyl-1-piperazinyl)benzoxazole (1n). Obtained as yellow oil, 70% yield from 2-amino-6-methylphenol. NMR ($CDCl_3$) δ: 2.36 (3H, s), 2.42 (3H, s), 2.53 (4H, t, J = 5 Hz), 3.73 (4H, t, J = 5 Hz), 6.83 (1H, d, J = 8 Hz), 7.06 (1H, t, J = 8 Hz), 7.19 (1H, d, J = 8 Hz). MS (EI) m/z 231 (M^+). HR-MS Calcd for $C_{13}H_{18}N_3O$: 232.1450. Found: 232.1448.

4.1.7. 2-(4-Methyl-1-piperazinyl)-5-trifluoromethylbenzoxazole (1k). This procedure illustrates the general synthetic method for **1c**, **1f**, **1l**, **1m**, **1o**, **1p**, **1q**, **1s**, **1t**, and **1v**. 2-Nitro-6-trifluoromethylphenol (0.88 g, 5.75 mmol) was dissolved in ethanol (30 ml), and 10% palladium–carbon (0.09 g) was added to the solution. The reaction mixture was stirred under a hydrogen atmosphere for 24 h, and the palladium–carbon was removed by filtration. The solution was concentrated in vacuo, then the crude 2-amino-6-trifluoromethylphenol was treated as described for the preparation of **1i** to afford **1k** as colorless needle, 21% yield from 2-nitro-4-trifluoromethylphenol, mp 72–73 °C (Et_2O–hexane). NMR ($CDCl_3$) δ: 2.36 (3H, s), 2.54 (4H, t, J = 5 Hz), 3.75 (4H, t, J = 5 Hz), 7.30 (2H, s), 7.57 (1H, s). MS (TSP) m/z 286 (M^++1). Anal. Calcd for ($C_{13}H_{14}N_3OF_3$): C, 54.74; H, 4.95; N, 14.73. Found: C, 54.63; H, 5.09; N, 14.49.

4.1.8. 5-Ethyl-2-(4-methyl-1-piperazinyl)benzoxazole (1c). Obtained as yellow oil, 98% yield from 4-ethyl-2-nitrophenol.[17] NMR ($CDCl_3$) δ: 1.24 (3H, t, J = 7 Hz), 2.35 (3H, s), 2.52 (4H, t, J = 5 Hz), 2.68 (2H, q, J = 7 Hz), 3.71 (4H, t, J = 5 Hz), 6.85 (1H, dd, J = 1, 8 Hz), 7.14 (1H, d, J = 8 Hz), 7.19 (1H, s). MS (EI) m/z 245 (M^+). HR-MS Calcd for $C_{14}H_{20}N_3O$(M^++1): 246.1606. Found: 246.1616.

4.1.9. 5-Methoxy-2-(4-methyl-1-piperazinyl)benzoxazole (1f). Obtained as yellow oil, 92% yield from 4-methoxy-2-nitrophenol. NMR ($CDCl_3$) δ: 2.35 (3H, s), 2.52 (4H, t, J = 5 Hz), 3.71 (4H, t, J = 5 Hz), 3.80 (3H, s), 6.58 (1H, dd, J = 3, 9 Hz), 6.92 (1H, d, J = 3 Hz), 7.12 (1H, d, J = 9 Hz). MS (TSP) m/z 248 (M^++1). HR-MS Calcd for $C_{13}H_{18}N_3O_2$(M^++1): 248.1399. Found: 248.1390.

4.1.10. 5-Aceto-2-(4-methyl-1-piperazinyl)benzoxazole (1l). Obtained as brown oil, 87% yield from 4′-hydroxy-3′-nitroacetophenone. NMR ($CDCl_3$) δ: 2.36 (3H, s), 2.54 (4H, t, J = 5 Hz), 2.62 (3H, s), 3.75 (4H, t, J = 5 Hz), 7.29 (1H, d, J = 8 Hz), 7.74 (1H, dd, J = 2, 8 Hz).

4.1.11. 5-Ethoxycarbonyl-2-(4-methyl-1-piperazinyl)benzoxazole (1m). Obtained as colorless needle, 90% yield from 4-ethoxycarbonyl-2-aminophenol,[18] mp 49–51 °C (Et_2O–hexane). NMR ($CDCl_3$) δ: 1.39 (3H, t, J = 7 Hz), 2.36 (3H, s), 2.53 (4H, t, J = 5 Hz), 3.74 (4H, t, J = 5 Hz), 4.37 (2H, q, J = 7 Hz), 7.26 (1H, d, J = 8 Hz), 7.80 (1H, dd, J = 2, 8 Hz), 8.03 (1H, d, J = 2 Hz). MS (TSP) m/z 290 (M^++1). Anal. Calcd for ($C_{15}H_{19}N_3O_3$-1/3H_2O): C, 61.00; H, 6.71; N, 14.23. Found: C, 60.97; H, 6.41; N, 14.30.

4.1.12. 7-Ethyl-2-(4-methyl-1-piperazinyl)benzoxazole (1o). Obtained as brown oil, 48% yield from 2-ethyl-6-nitrophenol.[19] NMR ($CDCl_3$) δ: 1.31 (3H, t, J = 8 Hz), 2.36 (3H, s), 2.54 (4H, t, J = 4 Hz), 2.81 (2H, q, J = 8 Hz), 3.73 (4H, t, J = 4 Hz), 6.86 (1H, d, J = 7 Hz), 7.09 (1H, t, J = 7 Hz), 7.20 (1H, d, J = 7 Hz). MS (EI) m/z 245 (M^+).

4.1.13. 7-Isopropyl-2-(4-methyl-1-piperazinyl)benzoxazole (1p). Obtained as yellow oil, 66% yield from 2-isopropyl-6-nitrophenol.[20] NMR ($CDCl_3$) δ: 1.35 (6H, d, J = 7 Hz), 2.36 (3H, s), 2.54 (4H, t, J = 5 Hz), 3.23 (1H, m), 3.73 (4H, t, J = 5 Hz), 6.88 (1H, m), 7.10 (1H, t, J = 8 Hz), 7.20 (1H, dd, J = 1, 8 Hz). FAB-MS m/z 260 (M^++1).

4.1.14. 7-Methoxy-2-(4-methyl-1-piperazinyl)benzoxazole (1q). Obtained as brown oil, 89% yield from 2-methoxy-6-nitrophenol.[21] NMR ($CDCl_3$) δ: 2.35 (3H, s), 2.52 (4H, t, J = 5 Hz), 3.74 (4H, t, J = 5 Hz), 3.97 (3H, s), 6.63 (1H, m), 7.00 (1H, m), 7.10 (1H, t, J = 9 Hz). MS (EI) m/z 247 (M^+).

4.1.15. 5,7-Dimethyl-2-(4-methyl-1-piperazinyl)benzoxazole (1s). Obtained as yellow oil, 73% yield from 2,4-dimethyl-6-nitrophenol.[22] NMR ($CDCl_3$) δ: 2.34 (6H, s), 2.36 (3H, s), 2.50 (4H, t, J = 4 Hz), 3.70 (4H, t, J = 4 Hz), 6.60 (1H, s), 7.00 (1H, s). FAB-MS m/z 246 (M^++1). HR-MS Calcd for $C_{14}H_{20}N_3O$(M^++1): 246.1609. Found: 246.1608.

4.1.16. 7-Ethyl-5-methyl-2-(4-methyl-1-piperazinyl)benzoxazole (1t). Obtained as yellow oil, 85% yield from 4-ethyl-2-methyl-6-nitrophenol. NMR ($CDCl_3$) δ: 1.31 (3H, t, J = 8 Hz), 2.34 (3H, s), 2.36 (3H, s), 2.54 (4H, t, J = 4 Hz), 2.81 (2H, q, J = 8 Hz), 3.73 (4H, t, J = 4 Hz), 6.60 (1H, s), 7.00 (1H, s). MS (TSP) m/z 260 (M^++1).

4.1.17. 7-Methoxy-5-methyl-2-(4-methyl-1-piperazinyl)benzoxazole (1v). Obtained as yellow oil, 93% yield from 2-methoxy-4-methyl-6-nitrophenol.[23] NMR ($CDCl_3$) δ: 2.34 (3H, s), 2.38 (3H, s), 2.51 (4H, t, J = 5 Hz), 3.72 (4H, t, J = 5 Hz), 3.95 (3H, s), 6.44 (1H, s), 6.80 (1H, s). MS (TSP) m/z 262 (M^++1). HR-MS Calcd for $C_{14}H_{20}N_3O_2$(M^++1): 262.1555. Found: 262.1559.

4.1.18. 5-Chloro-7-methyl-2-(4-methyl-1-piperazinyl)benzoxazole (1w). This procedure illustrates the general synthetic method for **1h**, **1j**, **1r**, **1u**, and **1x**–**z**. 4-Chloro-2-methyl-6-nitrophenol[24] (**5w**, 2.0 g, 10.7 mmol) was dissolved in ethyl acetate (60 ml), and 5% platinum on sulfide carbon (60 mg; Aldrich Chemical Co.) was added to the solution. The reaction mixture was stirred under hydrogen atmosphere for 24 h, and platinum on sulfide carbon was removed by filtration. The solution was concentrated in vacuo. The 1.7 g (10.7 mmol) of crude 2-amino-4-chloro-6-methylphenol was refluxed for 8 h with

potassium hydroxide (4.7 g, 84 mmol) and carbon disulfide (33 ml) in ethanol (100 ml). The reaction mixture was concentrated in vacuo, and 5 N aqueous hydrochloric acid (18 ml) and ethyl acetate (100 ml) were added to the residue. The organic layer was washed with water (100 ml), dried over $MgSO_4$, and concentrated in vacuo. 5-Chloro-2-mercapto-7-methylbenzoxazole (**7w**) was obtained as a pale-brownish solid and used in the next step without further purification. **7w** (0.2 g, 1.0 mmol) and methylpiperazine (0.5 ml, 4.5 mmol) were dissolved in dry toluene (15 ml), and the mixture was refluxed for 16 h. The solvent was removed under reduced pressure, and the residue was chromatographed on silica gel with dichloromethane–methanol (10:1) to give **1w** (270 mg, 84% from **5w**) as yellow solid, mp 62–64 °C (Et_2O–hexane). NMR ($CDCl_3$) δ: 2.36 (3H, s), 2.37 (3H, s), 2.53 (4H, t, $J = 5$ Hz), 3.72 (4H, t, $J = 5$ Hz), 6.81 (1H, d, $J = 2$ Hz), 7.14 (1H, d, $J = 2$ Hz). MS (TSP) *m/z* 266 (M^++1), 268 (M^++3). Anal. Calcd for ($C_{13}H_{16}N_3OCl$): C, 58.76; H, 6.07; N, 15.82. Found: C, 58.73; H, 6.12; N, 15.69.

4.1.19. 5-Fluoro-2-(4-methyl-1-piperazinyl)benzoxazole (1h). Obtained as colorless needle, 74% yield from 4-fluoro-2-nitrophenol, mp 116–117 °C (Et_2O–hexane). NMR ($CDCl_3$) δ: 2.35 (3H, s), 2.52 (4H, t, $J = 5$ Hz), 3.72 (4H, t, $J = 5$ Hz), 6.71 (1H, dt, $J = 2$, 9 Hz), 7.04 (1H, dd, $J = 2$, 9 Hz), 7.14 (1H, dd, $J = 4$, 9 Hz). MS (EI) *m/z* 235 (M^+). Anal. Calcd for ($C_{12}H_{14}N_3OF$): C, 61.26; H, 6.00; N, 17.86. Found: C, 61.21; H, 5.99; N, 17.87.

4.1.20. 5-Bromo-2-(4-methyl-1-piperazinyl)benzoxazole (1j). Obtained as colorless needle, 60% yield from 4-bromo-2-nitrophenol, mp 100–101 °C (Et_2O–hexane). NMR ($CDCl_3$) δ: 2.36 (3H, s), 2.47 (3H, s), 2.53 (4H, t, $J = 5$ Hz), 3.74 (4H, t, $J = 5$ Hz), 6.71 (1H, dt, $J = 2$, 9 Hz), 7.04 (1H, d, $J = 7$ Hz), 7.26 (1H, s), 7.28 (1H, d, $J = 7$ Hz). MS (TSP) *m/z* 235 (M^++1), 238 (M^++3). Anal. Calcd for ($C_{12}H_{14}N_3OBr$): C, 48.67; H, 4.76; N, 14.19. Found: C, 48.48; H, 4.66; N, 13.99.

4.1.21. 7-Chloro-2-(4-methyl-1-piperazinyl)benzoxazole (1r). Obtained as brown oil, 87% yield from 2-chloro-6-nitrophenol. NMR ($CDCl_3$) δ: 2.36 (3H, s), 2.54 (4H, t, $J = 5$ Hz), 3.76 (4H, t, $J = 5$ Hz), 7.00 (1H, dd, $J = 1$, 8 Hz), 7.09 (1H, t, $J = 8$ Hz), 7.23 (1H, dd, $J = 1$, 8 Hz). MS (EI) *m/z* 251 (M^+), 253 (M^++2).

4.1.22. 7-Chloro-5-methyl-2-(4-methyl-1-piperazinyl)benzoxazole (1u). Obtained as yellow plate, 96% yield from 2-chloro-4-methyl-6-nitrophenol,[25] mp 58–59 °C (Et_2O–hexane). NMR ($CDCl_3$) δ: 2.35 (3H, s), 2.36 (3H, s), 2.53 (4H, t, $J = 5$ Hz), 3.74 (4H, t, $J = 5$ Hz), 6.82 (1H, s), 7.02 (1H, s). MS (TSP) *m/z* 266 (M^++1), 268 (M^++3). Anal. Calcd for ($C_{13}H_{16}N_3OCl$): C, 58.76; H, 6.07; N, 15.81. Found: C, 58.88; H, 5.97; N, 15.93.

4.1.23. 5-Chloro-7-ethyl-2-(4-methyl-1-piperazinyl)benzoxazole (1x). Obtained as yellow powder, 55% yield from 4-chloro-2-ethyl-6-nitrophenol.[26] NMR ($CDCl_3$) δ: 1.29 (3H, t, $J = 7$ Hz), 2.36 (3H, s), 2.53 (4H, t, $J = 5$ Hz), 2.78 (2H, q, $J =$ Hz), 3.72 (4H, t, $J = 5$ Hz), 6.83 (1H, d, $J = 2$ Hz), 7.15 (1H, d, $J = 2$ Hz). MS (TSP) *m/z* 280 (M^++1), 282 (M^++3). HR-MS Calcd for ($C_{14}H_{19}N_3OCl$ (M^++1): 280.1217. Found: 280.1193.

4.1.24. 5,7-Dichloro-2-(4-methyl-1-piperazinyl)benzoxazole (1y). Obtained as yellow needle, 64% yield from 2,4-dichloro-6-nitrophenol, mp 106–107 °C (Et_2O–hexane). NMR ($CDCl_3$) δ: 2.36 (3H, s), 2.53 (4H, t, $J = 5$ Hz), 3.75 (4H, t, $J = 5$ Hz), 7.00 (1H, d, $J = 2$ Hz), 7.18 (1H, d, $J = 2$ Hz). MS (EI) *m/z* 285 (M^+), 287 (M^++2), 289 (M^++4). Anal. Calcd for ($C_{12}H_{13}N_3Ocl_2$): C, 50.37; H, 4.58; N, 14.68. Found: C, 50.10; H, 4.42; N, 14.44.

4.1.25. 5-Chloro-7-methoxy-2-(4-methyl-1-piperazinyl)benzoxazole (1z). Obtained as colorless solid, 70% yield from 4-chloro-2-methoxy-6-nitrophenol.[27] NMR ($CDCl_3$) δ: 2.32 (3H, s), 2.51 (4H, t, $J = 5$ Hz), 3.73 (4H, t, $J = 5$ Hz), 3.95 (3H, s), 6.61 (1H, d, $J = 2$ Hz), 6.97 (1H, d, $J = 2$ Hz). MS (TSP) *m/z* 282 (M^++1), 175 (M^++3).

4.1.26. 5-Amino-2-(4-methyl-1-piperazinyl)benzoxazole (1g). Compound **1g** was obtained by the catalytic hydrogenolysis of **1e** (26 mg, 0.1 mmol) using palladium–carbon (3 mg) in 1:1 mixture of ethyl acetate–ethanol (4 ml), 27% yield based on **1e**. NMR ($CDCl_3$) δ: 2.36 (3H, s), 2.56 (4H, t, $J = 5$ Hz), 3.64 (4H, t, $J = 5$ Hz), 6.45 (1H, dd, $J = 2$, 8 Hz), 6.91 (1H, d, $J = 2$ Hz), 7.33 (1H, d, $J = 8$ Hz). MS (EI) *m/z* 233 (M^++1).

4.2. Computational chemistry

4.2.1. Molecular modeling. Agonist/antagonist bound models of extracellular regions of the homopentameric guinea pig 5-HT_3 receptor were constructed by using HOMOLOGY module of Insight II and Cerius2 (Accelrys, San Diego, CA): An agonist bound model was built based on the crystal structure of AChBP complexed with a nACh receptor agonist, LOB (PDB entry 2BYS).[12] An antagonist bound model was formed from the crystal structure of AChBP with a nACh receptor antagonist MLA (PDB entry 2BYR).[12] The sequence of the guinea pig 5-HT_3 receptor A subunit was brought from GenBank (AAC06136). Sequence alignment between extracellular region of guinea pig 5-HT_3 receptor and AChBP was performed based on reported alignment results[7,28] by using Clustal W.[29] On the basis of this alignment, models of the 5-HT_3 receptor subunit were built by Insight II, and each model was then minimized in Cerius2 using the cff1.02 force field[30] by moving side chains alone. The pentamer models were generated by superimposing the models onto each protomer of AChBP and then were minimized by moving side chains alone.

4.2.2. Docking of 1a. Docking of **1a** was carried out using agonist bound model as docking template, because **1a** has a high ia value (0.62). Initial position

of **1a** in agonist bound model was determined by referring binding conformations of nACh receptor agonists to AChBP,[12,13] that is, an ammonium salt on the piperidinyl moiety, a Ph ring, and a carbonyl oxygen in LOB's structure were, respectively, replaced to the ammonium salt in the C2 piperadinyl substituent, the Ph ring, and the nitrogen atom in benzoxazole of **1a**. After an initial position of **1a** is determined, energy minimization was carried out by Cerius2 using the cff1.02 force field with moving **1a** and amino acids' side chains around **1a**.

4.3. Biology

4.3.1. Contraction Test.[9] Male Hartley guinea pigs weighing 500–600 g were sacrificed by exanguination, and the ileum was excised. Pieces (about 20 mm) of ileal longitudinal muscles were placed in a 5 ml organ bath containing Krebs–Henseleit solution aerated with 95% O_2 and 5% CO_2 at 37 °C. The composition of the solution was as follows (mM): NaCl 118, KCl 4.7, KH_2PO_4 1.19, $MgSO_4$ 1.2, $CaCl_2$ 2.54, $NaHCO_3$25, and glucose 10. The solution contained ritanserin (10^{-7} M) to block the 5-HT_2 receptor-mediated response. The preparations were allowed to equilibrate for at least 30 min under 0.5 g of tension. After equilibration, the preparations were repeatedly exposed to 3×10^{-7} M 5-HT for 60 min to desensitize the 5-HT_4 receptor. Test compounds were added to the bath, and contractions were recorded isometrically. The potencies of agonists were expressed as pD_2 values, that is, the negative logarithm of the molar concentration which produced 50% of the maximum contraction obtained from individual concentration–response curves. The ia of test compounds was expressed as the ratio between the maximum response to a test compound and that to 5-HT (10^{-5} M). To evaluate antagonistic activities of the partial agonists, the contractile responses after a single application at 10^{-5} M of 5-HT were obtained in the absence and presence of the test compounds for 20 min. The vehicle-treated preparation was used for a time-matched control. The 5-HT_3 antagonism of test compounds were defined as the ratio of the contractile response for 5-HT in the presence and absence of compounds.

4.3.2. 5-HT_3 receptor binding assay. The assay was performed according to the method of Kilpatrick et al.[31] Brain cortices were isolated from male Wistar rats (250–300 g), and a membrane fraction was prepared by standard techniques. The membrane fraction (0.04 mg) was incubated with 0.2 nM [^{3}H]GR65630 for 60 min at 22 °C. Membranes were collected by filtration and washed three times. The radioactivity on the filters was counted to determine [^{3}H]GR65630 specifically bound. Nonspecific binding was estimated in the presence of 1 mM ICS205-930. For obtaining K_i values, assays were carried out six times at each dose and displacement curves were fitted by nonlinear regression. IC_{50} values were obtained directly. K_i values were calculated from IC_{50} values by using the equation of Cheng and Prusoff.[32]

Supplementary data

Supplementary data associated with this article can be found, in the online version, at doi:10.1016/j.bmc.2007.02.054.

References and notes

1. Kilpatrick, G. J.; Bunce, K. T.; Tyers, M. B. *Med. Res. Rev.* **1990**, *10*, 441–475.
2. Sanger, G. J.; Nelson, D. R. *Eur. J. Pharmacol.* **1989**, *159*, 113–124.
3. Butler, A.; Hill, J. M.; Ireland, S. J.; Jordan, C. C.; Tyers, M. B. *Br. J. Pharmacol.* **1988**, *94*, 397–412.
4. Camileri, M.; Northcutt, A. R.; Kong, S.; Dukes, G. E.; McSorley, D.; Mangel, A. W. *Lancet* **2000**, *355*, 1035–1040.
5. For selected SAR based studies on the LGIC receptors, see: Glennon, R. A.; Dukat, M.; Liao, L. *Curr. Top. Med. Chem.* **2004**, *4*, 631–644; Dukat, M. *Curr. Med. Chem. Cent. Nerv. Syst. Agents* **2004**, *4*, 77–94.
6. Costa, V.; Nistri, A.; Cavalli, A.; Carloni, P. *Br. J. Pharmacol.* **2003**, *140*, 921–931.
7. Suryanarayanan, A.; Joshi, P. R.; Bikadi, Z.; Mani, M.; Kulkarni, T. R.; Gaines, C.; Schulte, M. K. *Biochemistry* **2005**, *44*, 9140–9149.
8. Sato, Y.; Imai, M.; Amano, K.; Iwamatsu, K.; Konno, F.; Kurata, Y.; Sakakibara, S.; Hachisu, M.; Izumi, M.; Matsuki, N.; Saito, H. *Biol. Pharm. Bull.* **1997**, *20*, 752–755.
9. Yamada, M.; Sato, Y.; Kobayashi, K.; Konno, F.; Soneda, T.; Watanabe, T. *Chem. Pharm. Bull.* **1998**, *46*, 445–451.
10. Sato, Y.; Yamada, M.; Yoshida, S.; Soneda, T.; Ishikawa, M.; Nizato, T.; Suzuki, K.; Konno, F. *J. Med. Chem.* **1998**, *41*, 3015–3021.
11. Yoshida, S.; Shiokawa, S.; Kawano, K.; Ito, T.; Murakami, H.; Suzuki, H.; Sato, Y. *J. Med. Chem.* **2005**, *48*, 7075–7079.
12. Hansen, S. B.; Sulzenbacher, G.; Huxford, T.; Marchot, P.; Taylor, P.; Bourne, Y. *EMBO J.* **2005**, *24*, 3635–3646.
13. Celie, P. H. N.; van Rossum-Fikkert, S. E.; van Dijk, W. J.; Brejc, K.; Smit, A. B.; Sixma, T. K. *Neuron* **2004**, *41*, 907–914.
14. Celite, P. H. N.; Klaassen, R. V.; van Rossum-Fikkert, S. E.; van Elk, R.; van Nierop, P.; Smit, A. B.; Sixma, T. K. *J. Biol. Chem.* **2005**, *280*, 26457–26466.
15. Spier, A. D.; Lummis, S. C. R. *J. Biol. Chem.* **2000**, *275*, 5620–5625.
16. Beene, D. L.; Brandt, G. S.; Zhong, W.; Zacharias, N. M.; Lester, H. A.; Dougherty, D. A. *Biochemistry* **2002**, *41*, 10262–10269.
17. Kano, F.; Yamane, K.; Yamashita, K.; Hosoe, K.; Kiyoshi, W. JP Patent, 64–6279, 1989.
18. Papenfuss, T. (Hoechst A-G, Fed. Rept. Ger.). US patent, 3929864, 1975.
19. Melvin, J. A.; Wendell, P. C. *J. Am. Chem. Soc.* **1943**, *65*, 2395–2399.
20. Kano, F.; Yamane, K.; Yamashita, K.; Hosoe, K.; Watanabe, K. *Eur. Pat. Appl.* **1988**, 253340.
21. Dwyer, C. L.; Holzapfei, C. W. *Tetrahedron* **1998**, *54*, 7843–7848.
22. Cross, G. G.; Fisher, A.; Henderson, G. N.; Smyth, T. A. *Can. J. Chem.* **1984**, *62*, 1446–1451.
23. Ford, R. E.; Knowles, P.; Lunt, E.; Marshal, S. M.; Penrose, A. J.; Ramsden, C. A.; Summers, A. J. H.;

Walker, J. L.; Wright, D. E. *J. Med. Chem.* **1986**, *29*, 538–549.
24. Gibson, G. P. *J. Chem. Soc.* **1925**, *127tl*, 42–48.
25. Clewly, R. G.; Cross, G. G.; Fischer, A.; Henderson, G. N. *Tetrahedron* **1989**, *5*, 1299–1310.
26. Schroetter, E.; Weuffen, W.; Herudek, D. *Pharmazie* **1974**, *29*, 374.
27. Backstrom, R.; Honkanen, E.; Pippuri, A.; Kairisalo, P.; Pystynen, J.; Heinola, K.; Nissinen, E.; Linden, I.; Mannisto, P. T.; Kaakkola, S.; Pohto, P. *J. Med. Chem.* **1989**, *32*, 841–846.
28. Brejc, K.; van Dijk, W. J.; Klaassen, R. V.; Schuurmans, M.; van der Oost, J.; Smlt, A. B.; Sixma, T. K. *Nature* **2001**, *411*, 269–276.
29. Thompson, J. D.; Higgins, D. G.; Gibson, T. J. *Nucleic Acid Res.* **1994**, *22*, 4673–4680.
30. Hwang, M. J.; Stockfisch, T. P.; Hagler, A. T. *J. Am. Chem. Soc.* **1994**, *116*, 2515–2525.
31. Kilpatrick, G. J.; Jones, B. J.; Tyers, M. B. *Nature* **1987**, *330*, 746–748.
32. Cheng, Y.-C.; Prusoff, W. H. *Biochem. Pharmacol.* **1973**, *22*, 3099–3108.